CURRENT TRENDS IN THE ANALYSIS OF POLYMER SHAPING OPERATIONS

by

Musa R. Kamal
Professor
Chemical Engineering Department
McGill University
Montréal, Québec H3A 2A7

and

Georges L. Bata
Director
Industrial Materials Research Institute
National Research Council Canada
75 De Mortagne Boulevard
Boucherville, Québec J4B 6Y4

Presented at the

European Meeting on Polymer Processing and Properties

Capri, Italy

June 12-16, 1983

Note au lecteur:

Les idées exprimées dans ce document sont celles de l'auteur (ou du contractant) et ne sont pas nécessairement partagées par l'Institut de génie des matériaux ou par le Conseil national de recherches Canada. L'auteur (ou le contractant) en assume l'entière responsabilité.

Si la demande est suffisante, des exemplaires supplémentaires de cet ouvrage pourront être disponibles dans la seconde langue officielle (français ou anglais).

Note to the reader:

The views expressed in this document are those of the author (or contractor) who assumes their full responsibility. They are not necessarily shared by the Industrial Materials Research Institute or the National Research Council of Canada.

If sufficient requests are received, a copy of this document will be made available in the other official language (French or English).

RÉSUMÉ

FORMAGE DES POLYMÈRES

Musa R. Kamal, *Dép. de génie chimique, université McGill, Montréal (Canada) et Georges L. Bata, Institut de génie des matériaux, Montréal, (Canada).

Dans tous les procédés de fabrication des plastiques, il faut une opération de formage afin de donner au matériau la forme et les dimensions voulues. Le formage est caractérisé par des combinaisons de déformations visco-élastiques et de transfert de chaleur qui sont généralement associées à la solidification du produit résultant de la coulée.

Le formage primaire comprend : a) des opérations bidimensionnelles, p.ex. le formage en filière, le calandrage et le revêtement, et b) des opérations de moulage tridimensionnelles. Les opérations bidimensionnelles sont soit du type continu, permanent (extrusion de films et de feuilles, revêtement de fils, revêtement de papier et de feuilles, calandrage, filage de fibres, extrusion de tuyaux et de profils, etc.), soit du type intermittent et au moulage par injection avec préplastification en mode alternatif. En général, les opérations de moulage sont intermittentes et de ce fait, ont tendance à présenter des conditions de régime transitoire. Le thermo-formage, le formage sous vide et les procédés similaires peuvent être considérés comme des opérations de formage secondaire, car elles ont habituellement

---

* Toute correspondance doit lui être adressée.

pour but de former en trois dimensions un corps qui a déjà été formé en deux dimensions.

Dans les opérations de formage, des phénomènes d'écoulement de fluide et de transfert de chaleur entrent en jeu simultanément ou à des moments différents. Dans les procédés bidimensionnels, la solidification suit généralement l'étape du formage, alors que dans les procédés tridimensionnels, la solidification et le formage ont tendance à se produire simultanément à l'intérieur du moule. Selon la nature du matériau, l'équipement et les conditions de traitement, les régimes d'écoulement sont habituellement des combinaisons d'écoulement de cisaillement, d'allongement et de compression associées à des écoulements intérieurs ou à surface libre.

Les facteurs thermo-mécaniques auxquels le polymère a été exposé pendant l'écoulement et la solidification sont à l'origine de la microstructure (distributions de morphologie, de degré de cristallisation et d'orientation) de l'article fabriqué. Les propriétés finales de l'article sont étroitement reliées à la microstructure. Le contrôle du procédé et de la qualité du produit doit par conséquent être basé sur une compréhension des interactions entre les propriétés des résines, le type d'équipement, les conditions d'exploitation, les facteurs thermo-mécaniques, la microstructure et les propriétés finales de l'article. On a fait appel à la modélisation mathématique et à la simulation sur ordinateur pour comprendre ces interactions.

Une telle approche prend de plus en plus d'importance en raison de l'utilisation grandissante des systèmes de conception et fabrication assistées par ordinateur (CFAO) dans le traitement des plastiques.

Nous traiterons des aspects susmentionnés relatifs au formage des polymères en insistant sur les perfectionnements récents en matière d'analyse et de simulation de certains procédés commerciaux importants, et en accordant l'importance nécessaire à la transformabilité, aux facteurs thermo-mécaniques, à la formation de la microstructure et aux propriétés du produit.

ABSTRACT

SHAPING OPERATIONS IN POLYMER PROCESSING

by

Musa R. Kamal,* Chemical Engineering Dept., McGill University, Montreal, Canada
and Georges L. Bata, Industrial Materials Research Institute, Montreal, Canada

In all plastics manufacturing processes, a shaping operation is required in order to impart to the material the desired shape and dimensions. Shaping involves combinations of viscoelastic deformations and heat transfer, which are generally associated with solidification of the product from the melt.

Primary shaping includes: (a) two-dimensional operations, e.g. die-forming, calendering and coating, and (b) three-dimensional molding operations. Two-dimensional processes are either of the continuous, steady state type (e.g. film and sheet extrusion, wire coating, paper and sheet coating, calendering, fiber spinning, pipe and profile extrusion, etc.) or intermittent as in the case of extrusions associated with intermittent extrusion blow molding and reciprocating screw injection molding. Generally, molding operations are intermittent, and, thus, they tend to involve unsteady state conditions. Thermo-forming, vacuum forming, and similar processes may be considered as secondary shaping operations, since they usually involve the reshaping of an already shaped form from a two-dimensional solid to a three-dimensional product.

Shaping operations involve simultaneous or staggered fluid flow and heat transfer. In two-dimensional processes, solidification usually follows the shaping process, whereas solidification

---

* To whom all correspondence should be addressed.

and shaping tend to take place simultaneously inside the mold in three-dimensional processes. Flow regimes, depending on the nature of the material, the equipment, and the processing conditions, usually involve combinations of shear, extensional, and squeezing flows in conjunction with enclosed (contained) or free surface flows.

The thermo-mechanical history experienced by the polymer during flow and solidification results in the development of microstructure (morphology, crystallinity, and orientation distributions) in the manufactured article. The ultimate properties of the article are closely related to the microstructure. Therefore, the control of the process and product quality must be based on an understanding of the interactions between resin properties, equipment design, operating conditions, thermo-mechanical history, microstructure, and ultimate product properties. Mathematical modeling and computer simulation have been employed to obtain an understanding of these interactions. Such an approach has gained more importance in view of the expanding utilization of computer aided design/computer assisted manufacturing (CAD/CAM) systems in conjunction with plastics processing.

The above aspects of polymer shaping will be treated, emphasizing recent developments relating to the analysis and simulation of some important commercial processes, with due consideration to processability, thermo-mechanical history, microstructure development, and product properties.

CURRENT TRENDS IN THE ANALYSIS OF POLYMER SHAPING OPERATIONS

Musa R. Kamal* and G.L. Bata**

*Chem. Eng. Dept., McGill University
Montreal, Canada H3A 2A7;
**Industrial Materials Research Institute
Montreal, Canada

INTRODUCTION

Polymer processing, in its most general context, involves the transformation of a solid (sometimes liquid) polymeric resin, which is in a random form (e.g. powder, pellets, beads), to a solid plastics product of specified shape, dimensions, and properties. This is achieved by means of a transformation process: extrusion, molding, calendering, coating, thermoforming, etc. The process, as demonstrated in Figure 1, in order to achieve the above objective, usually involves the following operations: solid transport, compression, heating, melting, mixing, shaping, cooling, solidification, and finishing. Obviously, these operations do not necessarily occur in sequence, and many of them take place simultaneously.

Shaping is required in order to impart to the material the desired geometry and dimensions. It involves combinations of viscoelastic deformations and heat transfer, which are generally associated with solidification of the product from the melt.

Shaping includes: (a) two-dimensional operations, e.g. dieforming, calendering and coating, and (b) three-dimensional molding and forming operations. Two-dimensional processes are either of the continuous, steady state type (e.g. film and sheet extrusion, wire coating, paper and sheet coating, calendering, fiber spinning, pipe and profile extrusion, etc.) or intermittent as in the case of extrusions associated with intermittent extrusion blow molding. Generaly, molding operations are intermittent, and, thus, they tend to involve unsteady state conditions. Thermoforming, vacuum forming, and similar processes may be considered as secondary shaping opera-

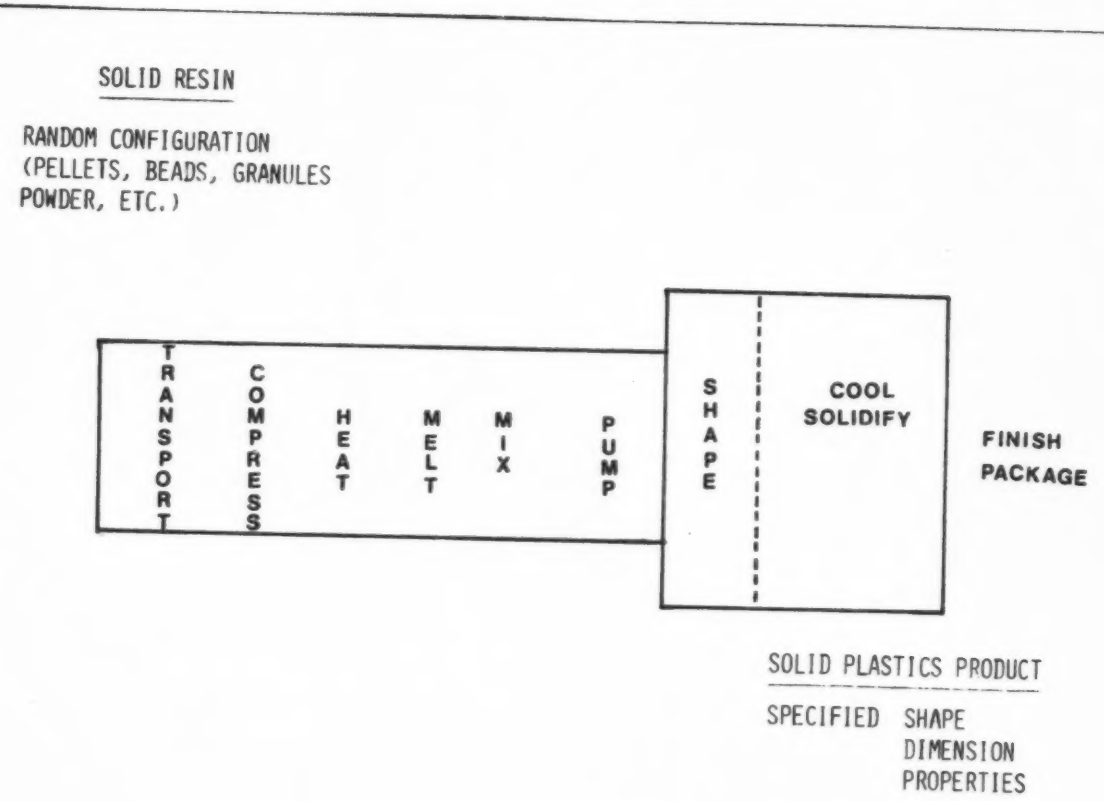

Figure 1: Sketch of a Typical Plastics Processing Sequence

tions, since they usually involve the reshaping of an already shaped form. In some cases, like blow molding, the process involves primary shaping (parison formation) and secondary shaping (parison inflation).

Shaping operations involve simultaneous or staggered fluid flow and heat transfer. In two-dimensional processes, solidification usually follows the shaping process, whereas solidification and shaping tend to take place simultaneously inside the mold in three-dimensional processes. Flow regimes, depending on the nature of the material, the equipment, and the processing conditions, usually involve combinations of shear, extensional, and squeezing flows in conjunction with enclosed (contained) or free surface flows.

The thermo-mechanical history experienced by the polymer during flow and solidification results in the development of microstructure (morphology, crystallinity, and orientation distributions) in the manufactured article. The ultimate properties of the article are closely related to the microstructure. Therefore, the control of the process and product quality must be based on an understanding of the interactions between resin properties, equipment design, operating conditions, thermo-mechanical history, microstructure, and ultimate product properties. Mathematical modeling and computer simulation have been employed to obtain an understanding of these interactions. Such an approach has gained more importance in view of the expanding utilization of computer aided design/computer assisted manufacturing /computer aided engineering (CAD/CAM/CAE) systems in conjunction with plastics processing.

The following discussion will highlight some of the basic concepts involved in plastics shaping operations. It will emphasize recent developments relating to the analysis and simulation of some important commercial processes, with due consideration to elucidation of both thermo-mechanical history and microstructure development. More extensive reviews of the subject can be found in standard references on the topic (1,2,3,4,5,6).

GENERAL APPROACH TO PROCESS MODELLING

As mentioned above, shaping operations involve combinations of fluid flow and heat transfer, with phase change, of a visco-elastic polymer melt. Both steady and unsteady state processes are encountered. A scientific analysis of operations of this type requires solving the relevant equations of continuity, motion, and energy (i.e. conservation equations).

In general tensorial formulation, the conservation equations, in differential form, are as follows:

Continuity

$$\frac{D\rho}{Dt} = -\rho(\nabla.\vec{v})$$

Momentum

$$\rho \frac{D\vec{v}}{Dt} = -\nabla P - \left[\nabla.\vec{\tau}\right] + \rho\vec{g}$$

Energy

$$\rho C_p \frac{DT}{Dt} = -(\nabla.\vec{q}) + \left(\frac{\partial \ln V}{\partial \ln T}\right) \frac{DP}{Dt} + (\vec{\tau}:\nabla\vec{v})$$

where ρ is the density, $\vec{v}$ is the velocity, P is the pressure, τ is the extra stress tensor, g is the gravitational acceleration, C_p is specific heat, T is temperature, $\vec{q}$ is the heat flux, V is the specific volume, and t is time.

Most work in the area of polymer processing has been limited to the treatment of one- or two-dimensional flow systems. Recently, more emphasis has been placed on the treatment of two-dimensional flow systems. Therefore, we shall present here the relevant equations for this case. The two dimensional equations, in Cartesian coordinates, take the following forms.

Continuity:

$$\frac{\partial \rho}{\partial t} = -\left[\frac{\partial}{\partial x}(\rho V_x) + \frac{\partial}{\partial y}(\rho V_y)\right]$$

Momentum:

$$\rho\left(\frac{\partial V_x}{\partial t} + V_x \frac{\partial V_x}{\partial x} + V_y \frac{\partial V_x}{\partial y}\right) = -\frac{\partial P}{\partial x} - \left(\frac{\partial \tau_{xx}}{\partial x} + \frac{\partial \tau_{xy}}{\partial y}\right) + \rho g_x$$

$$\rho\left(\frac{\partial V_y}{\partial t} + V_x \frac{\partial V_y}{\partial x} + V_y \frac{\partial V_y}{\partial y}\right) = -\frac{\partial P}{\partial y} - \left(\frac{\partial \tau_{xy}}{\partial x} + \frac{\partial \tau_{yy}}{\partial y}\right) + \rho g_y$$

Energy:

$$\rho C_p\left(\frac{\partial T}{\partial t} + V_x \frac{\partial T}{\partial x} + V_y \frac{\partial T}{\partial y}\right) = -\left(\frac{\partial q_x}{\partial x} + \frac{\partial q_y}{\partial y}\right)$$

$$-\left(\tau_{xx} \frac{\partial V_x}{\partial x} + \tau_{yy} \frac{\partial V_y}{\partial y}\right) - \tau_{xy}\left(\frac{\partial V_x}{\partial y} + \frac{\partial V_y}{\partial x}\right)$$

$$+\left(\frac{\partial \ln V}{\partial T}\right)_p \left(\frac{\partial P}{\partial t} + V_x \frac{\partial P}{\partial x} + V_y \frac{\partial P}{\partial y}\right)$$

Similar equations can be written in cylindrical or spherical coordinates.

In dealing with polymer processing operations, analysis of the shaping stage involves solving the above equations with appropriate initial and boundary conditions, in conjunction with realistic representation of material properties. Generally, none of these aspects is a simple task, and, therefore, many assumptions and approximations are employed.

Analytical solutions to the above equations exist only for the simplest cases of isothermal, incompressible, Newtonian, one-dimensional flow. In spite of this, first approximations are based on such assumptions, and the results obtained have been usually helpful in equipment and process design and optimization. Even when numerical methods are employed, solutions are not readily economically obtainable, and compromises are necessary. In many cases, convergence is not obtainable even at high cost. The current trend, however, is to analyze shaping operations as non-isothermal, visco-elastic two-dimensional flows, with compressible or incompressible materials, depending on the system. To achieve this, finite element techniques, which also have the advantage of adaptability to boundaries having complex shape, are becoming an important tool of analysis. However, limitations still exist, and a number of problems must be resolved before many important questions can be answered.

In view of the above complexities, no standard or general approaches have evolved yet for dealing with the shaping aspects of polymer processing. However, the following section outlines some of the methods most commonly used by polymer processing engineers.

(i) Equations of State. As mentioned above, the fluid is assumed to be incompressible in a large number of situations. However, in cases where density variations are important, as in the case of packing and solidification during injection molding, it is desirable to employ an appropriate equation of state to describe pressure-volume-temperature (P-V-T) variations. Three such equations have been found to be useful.

Spencer and Gilmore equation (7):

$$(P + \pi)\ (V - \omega) = RT$$

Breuer and Rehage equation (8):

$$V = V_o + \phi_o T - \frac{K_o}{a}\ (1 + bT)\ \ln(1 + aP)$$

Kamal and LeVan equation (9):

$$\rho = \rho_\infty + \left(\frac{\partial \rho}{\partial P}\right)_{P=o} T + (\alpha + \beta T)P + \tfrac{1}{2}(c + dt)P^2$$

In the above, $\pi, \omega, R, V_o, \phi_o, K_o, a, b, \rho_\infty, \alpha, \beta, c$, and d are constants.

(ii) Rheological Constitutive Equations. This represents one of the most complex issues involved in the analysis of polymer processing operations. The complexity is related to two aspects: (a) generally, equations that contain a description of the viscoelastic nature of polymer melts are quite complex mathematically, and (b) at the moment, there does not exist one rheological constitutive equation that can describe accurately all aspects of the viscoelastic behavior of polymer melts. In view of the above, polymer processing engineers have learned the art of rheological compromise.

The most commonly used rheological constitutive equations in conjunction with polymer melts are the Newtonian and Power Law models. Since most process models are based on one- or two-dimensional flow representations, these rheological equations take the following forms for two dimensional flow.

Newtonian.

$$\tau_{xy} = \eta\left(\frac{\partial V_y}{\partial x} + \frac{\partial V_x}{\partial y}\right)$$

$$\tau_{xx} = 2\eta \frac{\partial V_x}{\partial x}$$

$$\tau_{yy} = 2\eta \frac{\partial V_y}{\partial y}$$

Power Law.

$$\eta(\gamma) = m(\tfrac{1}{2} I_2)^{\frac{n-1}{2}} = m\left[\tfrac{1}{2}(\gamma_{xx}^2 + \gamma_{yy}^2 + 2\gamma_{xy}^2)\right]^{\frac{n-1}{2}}$$

where γ_{ij} refers to the rate of strain component.

There are many other more complex models that are commonly used in polymer processing analysis. Some of the subsequent discussion in this review will deal with the follow-

ing three fluids: the convected Maxwell fluid, the White-Metzner Model and the Criminale-Ericksen-Filbey (CEF) fluid. The tensorial forms of these models are listed below, and the important parameters for two-dimensional flow are given in the Appendix.

Maxwell:

$$\overline{\overline{\tau}} + \lambda_o \frac{D\overline{\overline{\tau}}}{Dt} = -\eta_o \overline{\overline{\gamma}}$$

White-Metzner (10):

$$\overline{\overline{\tau}} + \frac{\eta}{G} \frac{D\overline{\overline{\tau}}}{Dt} = -\eta \overline{\overline{\gamma}}$$

CEF Model (11):

$$\overline{\overline{\tau}} = \eta \overline{\overline{\gamma}} + \tfrac{1}{2}(\Psi_1 + \Psi_2)\{\overline{\overline{\gamma}} \cdot \overline{\overline{\gamma}}\} - \tfrac{1}{2}\Psi_1 \frac{D\overline{\overline{\gamma}}}{Dt}$$

The Maxwell model has a constant viscosity and first normal stress coefficient and zero second normal stress coefficient, and its elongational viscosity becomes infinite at some finite elongation rate. In the White-Metzner modification of this fluid, the viscosity is a function of the rate of strain. For the CEF model, the viscosity and the first and second normal stress coefficients depend on the magnitude of the rate of strain tensor

$$\left|\gamma\right| = \left[\tfrac{1}{2} I_2\right]^{\frac{1}{2}} = \left[\sum_{ij}\sum \gamma_{ij} \cdot \gamma_{ji}\right]^{\frac{1}{2}}$$

In addition to the above constitutive equations expressed in the differential form, there are a number of integral constitutive equations that have been found useful and convenient in a variety of processing situations. Some of these equations are listed below.

Lodge's Rubberlike model (12):

$$\vec{\vec{\tau}} = + \int_{-\infty}^{t} M(t-t') \vec{\vec{\gamma}}(t')\, dt'$$

K-BKZ model (13)

$$\vec{\vec{\tau}} = + \int_{-\infty}^{t} \left[M_1(t-t',I,II)\vec{\vec{\gamma}}(t') + M_2(t-t',I,II)\{\vec{\vec{\gamma}}(t').\vec{\vec{\gamma}}(t')\} \right] dt'$$

(iii) Heat Transfer and Crystallization. Heat transfer is a critical aspect of plastics shaping, since the cooling or solidification time usually represents the longest proportion of the processing sequence and since the optimization of cooling rates is essential for controlling the rheological behavior during processing and the ultimate product properties. The treatment of heat transfer is based on the solution of the equation of energy, in conjunction with the equations of continuity and motion. In general, viscous dissipation is an important factor, especially at high processing speeds, due to the large viscosity of polymer melts. The boundary conditions usually reflect the cooling or heating conditions at the interfaces between the polymer and surrounding solid, liquid, or gaseous boundaries. Radiation can be an important factor as a heating source in some processes like thermoforming and blown film embossing, or as heat loss to the environment in many other situations. The treatment of convective heat transfer coefficients and radiation effects follows standard engineering procedures, and is well covered in standard polymer processing references (1-6).

One of the important areas involving heat transfer in polymer processing relates to heat generation or loss in the bulk of the material as a result of crystallization, melting, or chemical reaction as in the case of curing. In general, the above phenomena can be treated using approximately the same approach. In the following discussion, we shall concentrate on the analysis of heat transfer accompanied with crystallization in partially crystalline polymers. The treatment of melting is usually well covered in works dealing with melting during extrusion (14). Heat transfer in reactive thermosetting systems has been also discussed elsewhere (15). The approach discussed below incorporates the effects of both crystallization and the variation of the specific heat of each of the phases with temperature. Moreover, it permits the estimation of crystallinity development during processing (16).

A typical curve showing the dependence of the specific heat of a crystallizing polymer on temperature is shown in Figure 2. Assuming that the specific heats of the melt and the solid are independent of the cooling process, within the solidification range, the latent heat of solidification is

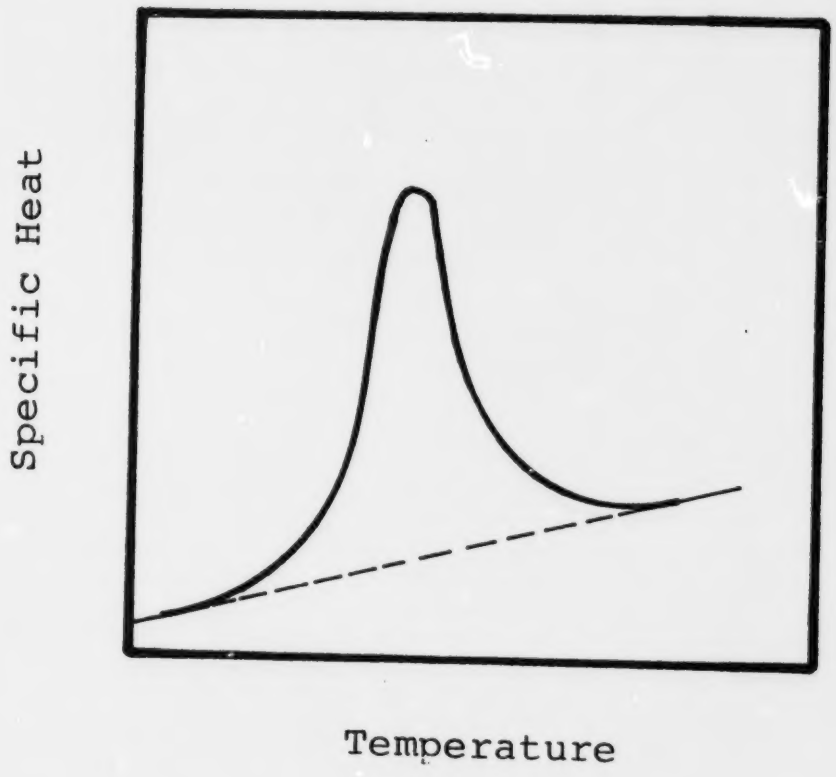

Figure 2: Typical DSC Scanning Curve for Specific Heat of a Crystallizing Polymer

included in the specific heat as follows:

$$C_p = C'_p + \frac{d\lambda c}{dT} = C'_p + \lambda_{pc} \frac{dx}{dt}$$

where C_p is the measured specific heat of the crystallizing melt, C_p' is the specific heat obtained by interpolation on the baseline, λ_c is the heat of crystallization released by the sample, λ_{pc} is the heat of fusion of the pure crystal, and X is the degree of crystallinity. Thus, it is important to follow the development of crystallinity in order to calculate the specific heat at any desired temperature during the process.

Nakamura et. al. (17) developed a procedure based on the Avrami equation, which was modified to apply to nonisothermal crystallization. The fundamental equation was written on the basis of isokinetic conditions:

$$X(t) = 1 - \exp\left[-\left(\int_0^t k(T)d\tau\right)^n\right]$$

where X(t): degree of phase transformation at time t.
n: Avrami index determined in isothermal experiments

$K(T) = \{k(T)\}^{\frac{1}{n}}$ where k(T) is the Avrami isothermal rate constant. From this model, nonisothermal crystallization can be analyzed in terms of data from isothermal crystallization experiments. The Avrami equation has the form:

$$X(t) = X(\infty)\left[1 - \exp\left(k(T)t^n\right)\right]$$

where $X(\infty)$ refers to the fact that the sample will reach a limiting crystallinity level. $X(\infty)$ will depend on temperature, and is below 1.0. It can be obtained from quenching experiments (16).

Figures 3 and 4 show comparisons between calculated and experimental temperature and crystallinity profiles obtained for the cooling of high density polyethylene is a static mold (16). The agreement is quite good. A similar approach, employing a somewhat different nonisothermal crystallization model, has been proposed by Dietz (18).

(iv) Numerical Methods. The formulation of polymer shaping problems, consisting of the continuity, momentum, and energy equations results in a system of multiple, simultaneous,

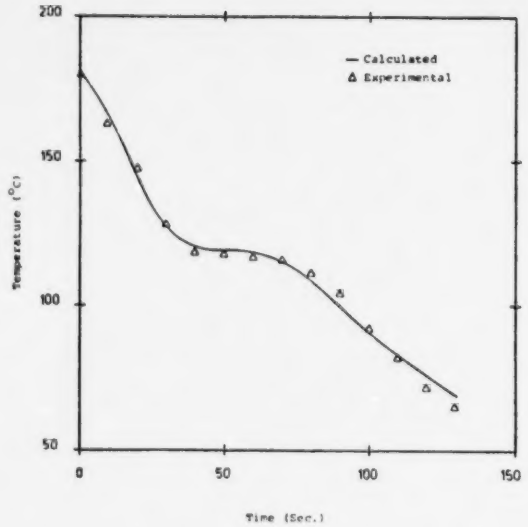

Figure 3: Temperature Profile During Static Cooling Experiment (16)

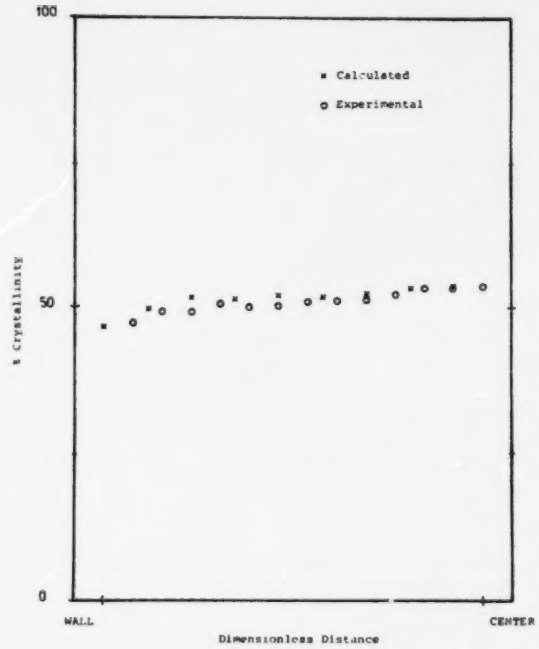

Figure 4: Crystallinity Profile During Static Cooling Experiment (16)

coupled, non-linear partial differential equations, which can only be solved by a numerical technique. Generally, the numerical techniques employed are based on finite difference or finite element methods.

When transient and inertial terms are neglected and when only simple, regular boundaries are involved, it is possible to employ an inexpensive explicit finite difference scheme. In some cases, involving simple shapes, a Marker-and-Cell technique may be used to treat free surface and transient flows (19). However, when the unsteady state terms of the momentum equations are included, it is necessary to use implicit finite difference equations because of the restriction on the time step due to the usually low Reynolds numbers. In this case, it might be more advisable to use finite element techniques.

Finite element techniques are finding wider applications, especially in systems involving free surface flows and complex geometries. For example, they have been used to study phenomena like die swell and entry and exit flows, in addition to molding situations involving complex molds and weld lines (20-26). One of the problems associated with these methods relates to the lack of convergence at Deborah Numbers ($\lambda\dot{\gamma}$ where λ is the characteristic time of the material and $\dot{\gamma}$ is the rate of deformation) exceeding unity. Recently, however, a number of workers have obtained convergence at Deborah numbers approaching 5.0 (23,27). Wang and Co-workers (26) have reported convergence for much higher Deborah numbers, employing a Leonov constitutive equation.

The use of finite element methods has also gained popularity because of the expansion in using CAD/CAM/CAE systems that incorporate three dimensional representation of objects having complex surface geometry.

EXAMPLES OF POLYMER SHAPING OPERATIONS

The remaining sections of this review outline the features of various models describing four typical plastics shaping operations. Two of the selected operations are basically continuous, steady state operations employed in generating two-dimensional (cross-section control) polymeric products: calendering for the production of film and sheet and wire coating for applying an annular coating over a cylindrical wire. The other two operations represent intermittent, unsteady state shaping operations for the manufacturing of three-dimensional objects: extrusion blow molding for the production of hollow containers and injection molding, which is the most important commercial process for the production of three-dimensional plastics articles. The discussion outlines the basic principles relating to the four operations and reviews

recent developments regarding the analysis and modeling of the phenomena involved.

CALENDERING

Calendering is a continuous, steady state process involving a pair of corotating heated rolls. The system is usually fed with a thermoplastic melt which is squeezed into a thin film or sheet at the outlet end. A sketch of the process is shown in Figure 5. The diameters and temperatures of the two rolls are not always equal.

The relevant equations for flow between narrow calendars, when coupled with the lubrication approximation, reduce to the following forms:

Continuity:

$$Q = 2 \int_o^h V_x dy$$

Momentum:

$$\frac{\partial P}{\partial x} = \frac{\partial}{\partial y} (\tau_{yx})$$

Boundary Conditions

$$\begin{array}{llll} \text{at the point of contact} & y = H & P = 0 & \\ \text{at the leave-off point} & y = H_1 & P = 0 & , \quad \frac{dP}{dx} = o \\ \text{at the upper cylinder} & y = h^1 & u = U_1 & \\ \text{at the lower cylinder} & y = -h & u = U_2^1 & \end{array}$$

The early analysis of calendering was developed by Gaskel (28) and McKelvey (2) for Newtonian and Power Law fluids. The isothermal flow analysis for a Newtonian fluid yields the following pressure profile for rolls of equal diameter and velocity.

$$P = \frac{\mu U}{Ho} \left(\frac{9R}{32Ho}\right)^{\frac{1}{2}} \left[g(\rho,\lambda) + c \right]$$

$$g(\rho,\lambda) = \left[\frac{\rho^2 - 1 - 5\lambda^2 - 3\lambda\rho^2}{(1 + \rho^2)^2} \right] \rho + (1 - 3\lambda^2) \tan^{-1} \rho$$

$$C \approx 5\lambda^3$$

$$\rho = \frac{x}{\sqrt{2RH_o}} \qquad ; \qquad \lambda^2 = \frac{x_1^2}{2RH_o}$$

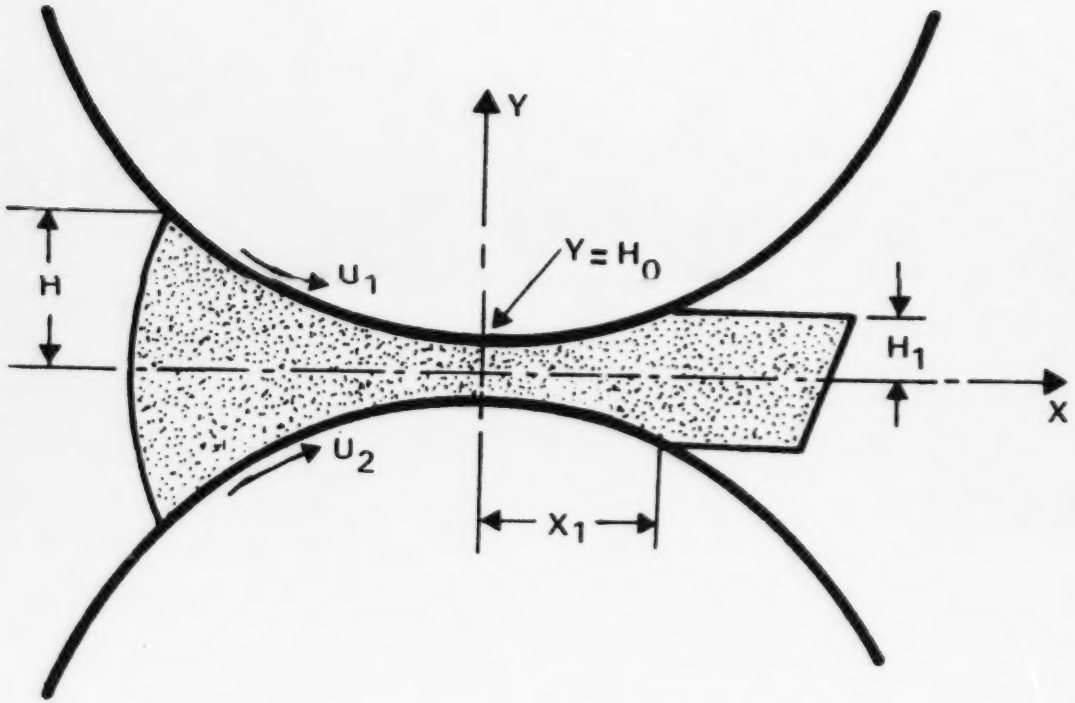

Figure 5: Notation for the Flow Analysis in the Gap between Two Rotating Calendar Rolls

In the above equations, P is the pressure, U is the velocity of the roll, and μ is the Newtonian viscosity of the fluid. The solution employs the lubrication assumption and assumes a no-slip condition. It yields a maximum pressure, P_{max}, at a point located at $-\lambda$ from the nip.

$$P_{max} = P(-\lambda) = \frac{5\mu U\lambda^3}{H_o} \left(\frac{9R}{Ho}\right)^{\frac{1}{2}}$$

and shows that the pressure at the nip is equal to half of the maximum pressure. Typical pressure profiles are shown in Figure 6 (29). The plots also show the effect of the Power Law index, n.

The velocity distribution for the system is given by the following equations:

$$\frac{V_x}{U} = \frac{2 + 3\lambda^2(1-\eta)^2 - \rho^2(1-3\eta^2)}{2(1 + \rho^2)}$$

where $\eta = \frac{y}{h}$

A typical velocity profile is shown in Figure 7 (2).

Alston and Astill (30) developed a calendering model for a "tanh" model fluid

$$\eta = A - B \tanh \left(\frac{\dot{\gamma}}{k}\right)^n$$

where A,B,k, and n are constants. Chung (31) carried out a similar analysis for a Bingham plastic fluid.

Recently, Vlachopoulos and Hrymak (32) extended the McKelvey and Gaskell analysis to allow for temperature rise due to viscous dissipation and for slip of the Power Law fluid at the rolls. They observed that the incorporation of slip yielded improved agreement between model predictions and experimental data for polyvinyl chloride. In more recent work, Kirpassidis and Vlachopoulos (29) and Mitsoulis, Vlachopoulos and Mirza (27) employed finite element methods to analyze the isothermal and non-isothermal two-dimensional calendering of Newtonian and Power Law fluids. The results showed that recirculating flow occurs in the entry, while flow becomes parallel in the vicinity of the minimum gap width. Figure 8 depicts the temperature development in a typical calender gap of a Power Law fluid (27). Mitsoulis, et. al. (27) have improved the

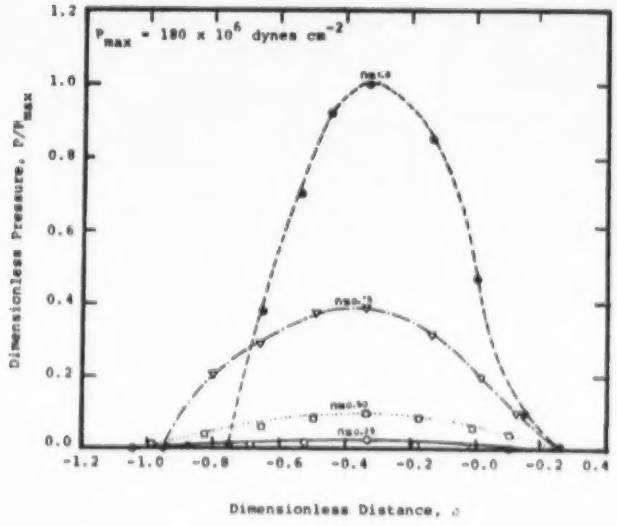

Figure 6: Effect of Power Law Index on Pressure Distribution in Calendering (29)

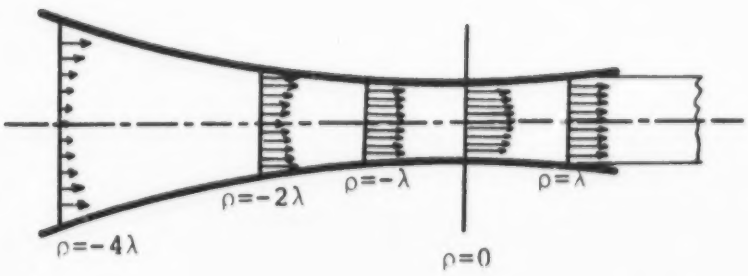

Figure 7: Velocity Profiles in Calendering ($\lambda^2 = 0.10$) for Isothermal Newtonian Flow (2)

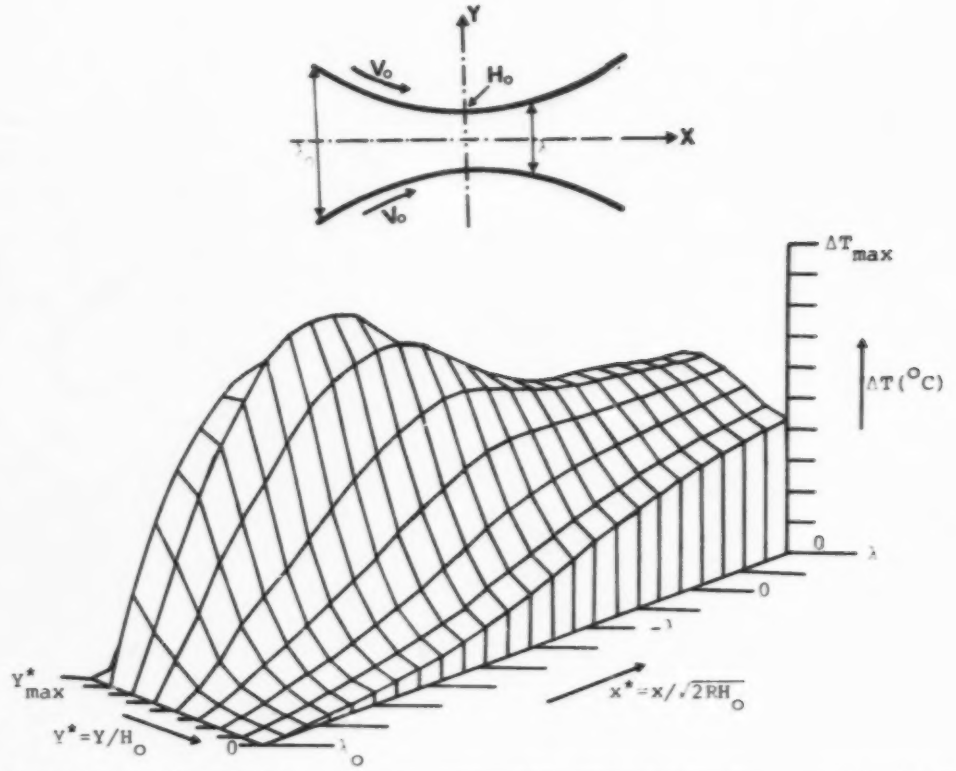

Figure 8: Temperature Distribution in the Calendering Gap (27)

stability of the solution of the non-isothermal problem by employing an "upwind" scheme. Moreover, they extended the finite element treatment to the analysis of the flow of a CEF viscoelastic fluid between parallel plates and the entry zones.

WIRE COATING

The wire and cable coating process is an extrusion operation which involves the coating of wires of various diameters with polymers in order to provide protection, insulation, and other desirable properties. The wire is fed to a crosshead die which leads to a guider tube. As the wire exits through the guider tip and enters the die forming regions, the polymer melt coats the wire circumferentially. The polymer is supplied to the die in molten form through the use of an extruder.

There are two basic wire coating die designs. These are known industrially as "tube type" and "pressure type" dies. In the first type, the coating is extruded in the form of a cylindrical tube, which is later drawn onto the moving wire, either by vacuum or by the pull of the wire, after the wire and the tube emerge separately from the die. In pressure dies, the wire contacts the pressurized molten polymer within the die, as shown in Figure 9. Both the wire and the polymer emerge simultaneously as coated wire from the die.

Both of the above die configurations can be used effectively for low speed wire coating. In the case of high speeds, the pressure type die is preferred, since it takes advantage of the wire drag and, therefore, requires lower operating pressures. At high wire speeds (4,000-5,000 ft/min), surface roughness and melt fracture are encountered.

Carley (34) and McKelvey (2) proposed the treatment of an idealized isothermal wire coating process for Newtonian fluids by addition of the contributions of drag and pressure flow in cylindrical annuli. Under these conditions, the overall flow rate, Q, is given by

$$Q = \frac{V_w WH}{2} + \frac{WH^3 \Delta P}{12 \mu L}$$

and

$$\Delta P = \frac{6 \mu L V_w (2h-H)}{H^3}$$

where V_w is the wire velocity, W is the mean circumference of the annular space, H is the size of the annular gap, ΔP is the applied pressure, L is the contact length between the wire and melt inside

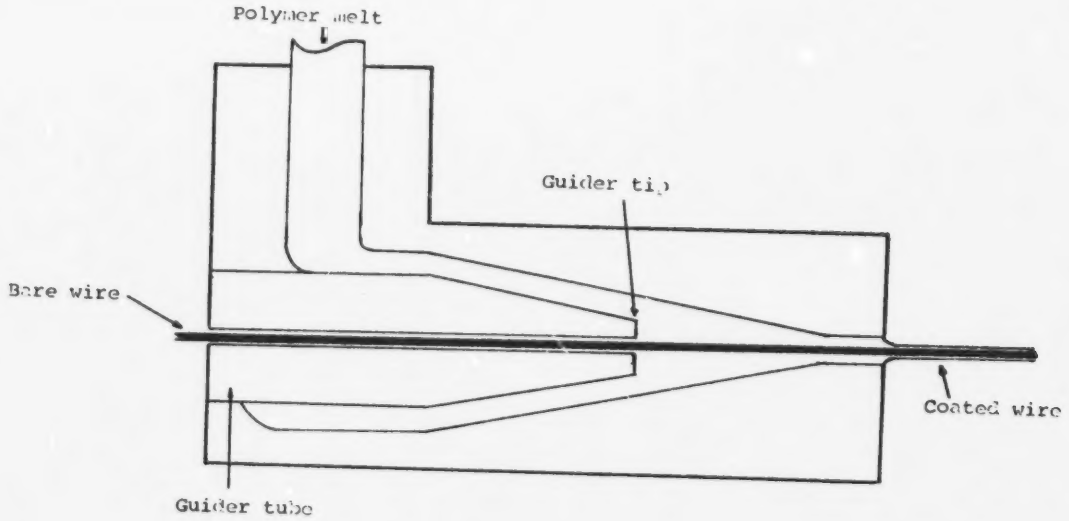

Figure 9: Pressure Type Wire Coating Die

the die, and μ is the Newtonian viscosity. Han and Rao (35) extended the above treatment to Power Law fluids. They divided the flow regime into two radial zones, one on each side of the point at which the maximum velocity occurs, $r/R_o = \lambda$, where R_o is the outer radius of the annulus. The expression for the volumetric flow rate, Q, becomes

$$Q = \pi R_o^2 (\lambda^2 - k^2) V_w + \pi R_o^3 \left(\frac{R}{2k} \frac{dP}{dz}\right)^s \int_k^1 \frac{(\lambda^2 - \xi^2)^{s+1}}{\xi^s} d\xi$$

where k is R_i/R_o with R_i being the inside radius of the annulus, s is 1/n where n is the Power Law index, ξ is the dimensionless radial position (r/R_o), and $\frac{dP}{dz}$ is the axial pressure gradient. The solution produces expressions for velocity distributions in the two radial zones, and it is necessary to employ a numerical technique to obtain λ by solving the equation for the identity of the velocity at the interface of the two zones. Typical results for the dependence of flow rate on wire speed and pressure gradient are shown in Figure 10 (5).

Carley, Endo, and Kranz (36) have obtained a finite difference solution for the two-dimensional (axial and radial) steady flow of an incompressible non-Newtonian fluid in both the tapered and die sections of the process. Their model employs a temperature and shear rate dependent viscosity and deals with both the isothermal and adiabatic situations. In order to avoid stability problems, they dropped the term $v_r \left(\frac{\partial T}{\partial r}\right)$ from the energy equation. Typical calculated temperature and velocity distributions in the tapered section of a commercial die, operating adiabatically with low density polyethylene at 4,000 ft/minute, are shown in Figures 11 and 12 (36). Similar solutions were obtained for a Power Law fluid by Vergnes (37). Fenner (38) and Fenner and Nadiri (39) employed finite element methods to solve a similar problem under isothermal conditions, employing the lubrication approximation. Basu (40) employed a finite difference scheme to solve coextrusion wire coating problems under non-isothermal conditions, but employing only one velocity component in the solution.

Although the lubrication approximation is helpful in cases involving small gap and taper angles, the procedure does not yield a clear and accurate description of stress distributions and irregularities that might lead to effects like melt fracture. Caswell and Tanner (41) have developed a finite element scheme to solve the relevant equations of change, without the lubrication approximation, in commercial wire coating dies. Since such dies usually include complex and changing geometries and involve abrupt changes in boundary conditions, the finite element method appears to be most

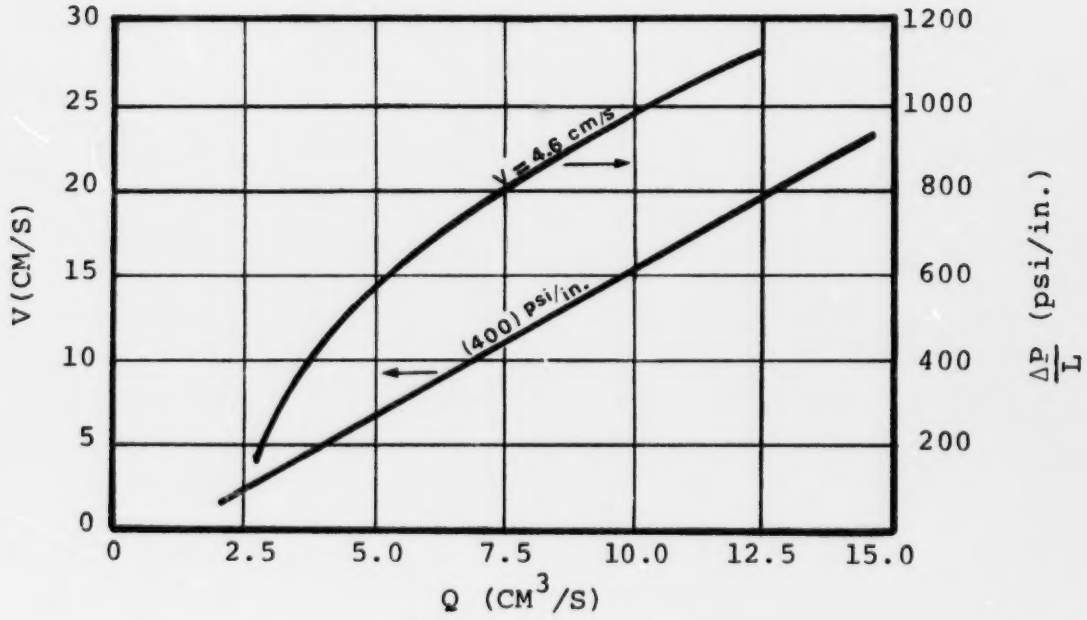

Figure 10: Calculated Effects of Wire Speed and Extrusion Pressure on Flow Rate of HDPE at 190°C. (5)

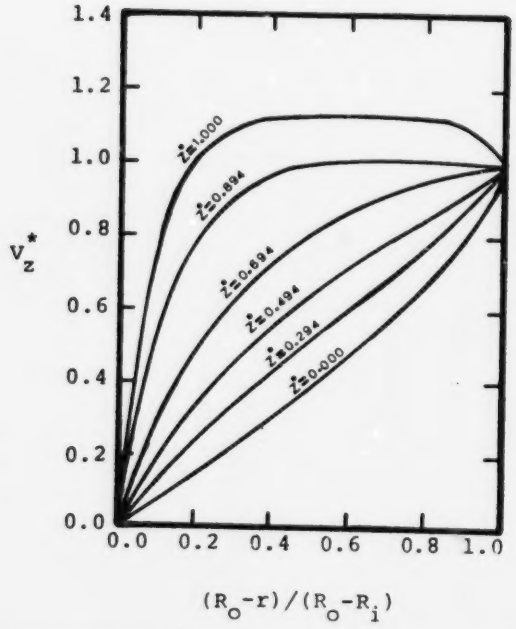

Figure 11: Velocity Profiles at Selected Axial Positions in LDPE Wire Coating Reference Velocity: 4000 ft/min. (36)

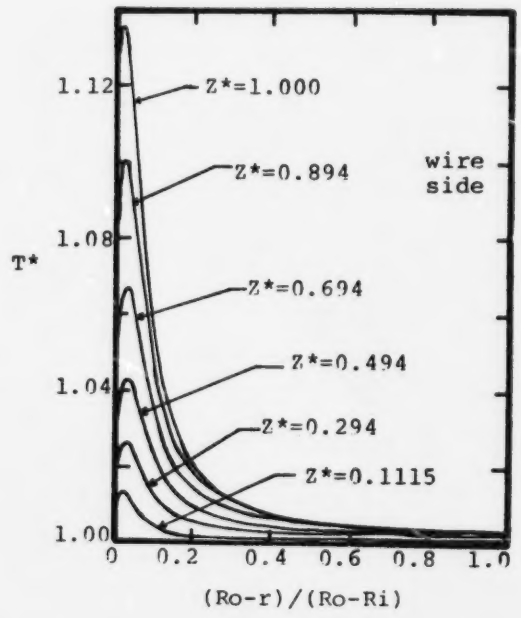

Figure 12: Temperature Profiles for LDPE at Wire Speed of 4000 ft/min. Reference temperature is 500°K (36)

suited for dealing with the wire coating problem. The application of this technique to isothermal Newtonian fluids shows circulation patterns in the area where die geometry changes, as indicated by the streamlines shown in Figure 13 (42). It has been possible to model isothermal pressure-type wire coating systems with this technique over a broad range of commercial operating speeds, for both Newtonian and Power Law fluids (42). However, instabilities in temperature predictions when nonisothermal solutions were attempted. The same approach was employed by Viriyaynthakorn and Deboo (43) for the analysis of tube-type wire coating dies, in conjunction with a generalized Newtonian fluid. An iterative procedure was employed to determine the shape of the unknown draw-down surface and the initial polymer-wire contact point. Typical stream lines for this situation are shown in Figure 14 (43).

BLOW MOLDING

Blow molding is the preferred commercial process for the production of hollow plastics containers. Extrusion blow molding consists of the following basic steps: (1) the extrusion of a molten plastic tube, "parison", from an annular die, (2) the clamping of the parison between the ends of a mold having the deisred shape, (3) the introduction of compressed air to inflate the parison so that it contacts the cold walls of the mold where it solidifies, and (4) the opening of the mold and ejection of the molding, when it has reached an acceptable level of rigidity. The cycle is repeated to produce identical articles. Blow molded articles cover a broad range of bottle shapes and sizes and include containers as large as 55 gallon drums.

Depending on the thermal stability of the material, the extrusion process can be continuous or intermittent. The former is the preferred technique with material having lower stability. Intermittent extrusion can employ either a reciprocating screw or an independent ram.

As a result of both parison swell and sag and the design characteristics of commercial containers, it is necessary to continually adjust the extrusion rate and/or parison thickness during extrusion. This is accomplished with the aid of parison programming, which involves movement of a mandrel to vary the size of the die opening or the control of the movement of the screw or the ram in intermittent blow molding. New machines employ electronic parison programming.

Injection blow molding offers the advantage of accurate dimensional control, elimination of scrap, and the molding of threads before blowing. A preform is injection molded over a rod, then the preform is introduced to the blow molding machine, where it is blown to the desired shape. Stretch blow molding is a process

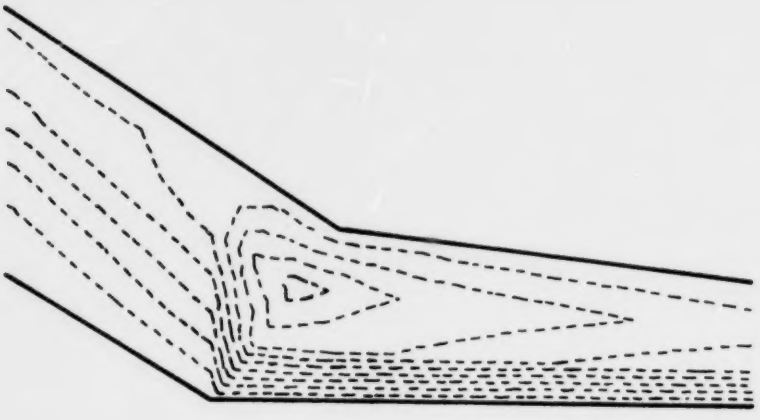

Figure 13: Calculated Streamlines and Circulation in Wire Coating Dies for A Newtonian Fluid ; Finite Element Method. (42)

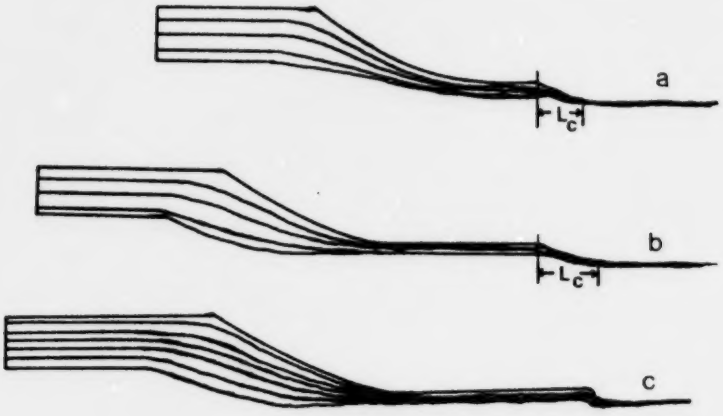

Figure 14: Streamlines Determined by Finite Element Analysis of Tube Type Coating Dies (43)

(a) Die A , no vacuum
(b) Die B , no vacuum
(c) Die C , high vacuum

whereby biaxial orientation (in the axial and radial directions) is optimized to yield desirable mechanical, optical, barrier and other physical-chemical properties. This process may be employed in conjunction with either extruded or injection molded parisons.

The optimization of the cooling system is an important aspect of blow molding, since it influences greatly production rates, production costs, and product quality. While high cooling rates (by employing refrigerated fluids) are desirable for high production rates, they could lead to frozen stresses and deficiencies in the product.

The shape and dimensions of the parison are the result of complex interactions between the molten polymer, which has been formed and shaped under the influence of thermal and mechanical conditions that exist in the die, and the thermo-mechanical conditions that influence the melt after it leaves the die. Parison swell is obtained as a result of exit phenomena and processes whereby the viscoelastic melt revovers from the shear and normal stresses which it experiences in the die. Sag or drawdown results from the action of gravity on the parison.

In a recent study, Orbey (44), evaluated the effects of die geometry on the isothermal swell and combined swell and sag for a variety of polyethylene blow molding resins. She discovered that diameter swell is highest for converging dies and lowest for diverging dies, while straight dies show intermediate swell between these extremes. The situation is not so clear for thickness swell, although it appears that converging dies exhibit somewhat higher thickness swell. The results indicate that the equilibrium diameter swell ratio, B_1, may be expressed in terms of the weight swell ratio, B_w, and the thickness swell ratio, B_2, according to the following relationship (45,46):

$$B_1 = AB_w^a = A(B_1B_2)^a$$

where A and a are constants depending on both the resin and geometry of the die. Generally, A is close to unity, while a is in the range 0.2 - 0.6. In the above:

$$B_1 = D_{o,e}/D_{o,d}$$

$$B_2 = G_e/G_d$$

$$B_w = B_1B_2$$

where $D_{o,e}$ is the outside diameter of the parison, $D_{o,d}$ is the out-

side diameter of the annular die, G_e is the thickness of the parison, and G_d is the annular gap at the die exit. It should be emphasized that the above relationship applies to equilibrium die swell, since swell is a transient phenomenon (45,47,48).

Conventionally, researchers have employed the parison pinch-off mold to determine the diameter swell characteristics of blow molding parisons (46,49,50). However, cinematographic studies have shown that this technique is not necessarily accurate (51).

Kamal, et. al. (52,53) have employed the approach proposed by Ajroldi (54) to estimate the dimensions of the parison under the combined effects of swell and sag. According to this approach, the area of a differential ith element of the parison (see Figure 15), $A^i(z,t)$, is

$$A^i(z,t) = \pi\left[B_1(t)D_{o,d} - B_2(t)G\right]\left[B_2(t)G\right]$$

where, t, refers to time and the transient nature of swell, and z is the axial distance below the die. Under the influence of sag, the area becomes $A_s^i(t)$, where

$$\ln A_s^i(t) = \ln A^i(t) - gJ(t)\{\Sigma W^i(t)\}/A_s^i(t)$$

where g is the gravitational constant, J(t) is the tensile compliance, and $W^i(t)$ is the weight of the ith pillow. The summation is taken to represent the weight of the elements below the its pillow. Kamal et. al. (52,53) obtained good agreement between calculated and measured parison diameters, as shown in Figure 16 (53). Similar agreement has been obtained for parison thickness and length.

Orbey (44) has proposed a somewhat similar model for the treatment of combined swell and sag in isothermal parisons. She bases her model on Lodge's rubber-like liquid model (12), which incorporates the relaxation spectra of the melt.

The shape of the parison at the end of extrusion tends to be circular. During the clamping stage, the parison is deformed both at the top and at the bottom. Fukase and coworkers (55) proposed equations for the estimation of the profile made by the outer surface of the parison during inflation. On the basis of this approach, it is possible to estimate the distribution of parison thickness in both the axial and circumferential directions (52,52).

More elaborate models describing the behavior of the parison formation stage (56) and the inflation stage (56-58). However,

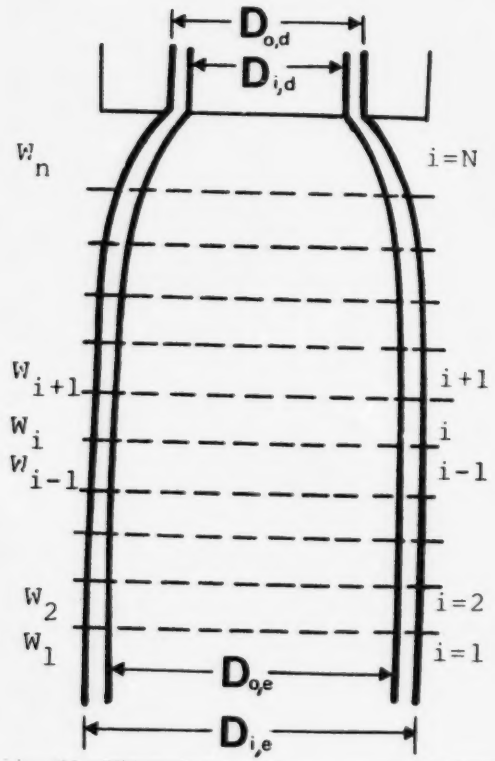

Figure 15: Schematic Diagram of Parison Segments During Extrusion

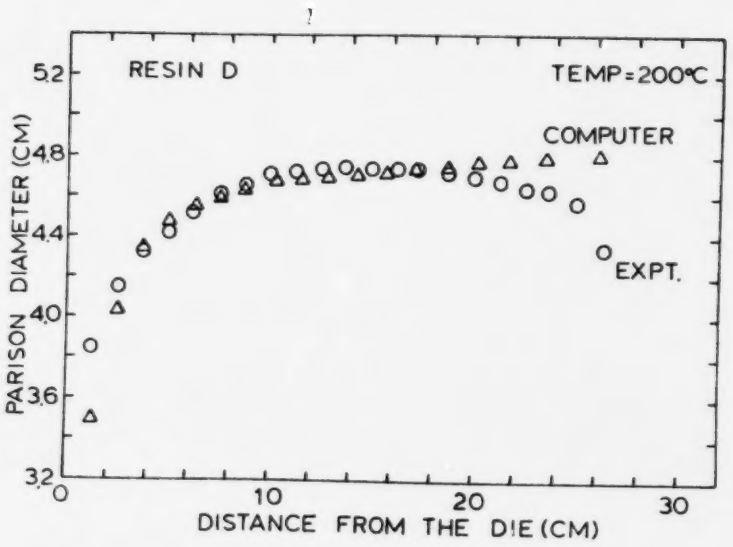

Figure 16: Comparison of Calculated and Experimental Parison Diameter Distributions for HDPE (53)

the predictions of these models have not been compared in sufficient detail to experimental data. In the following, we outline the model proposed by Ryan and Dutta (BM14).

According to the technique proposed by Ryan and Dutta (56), if the curvature of the surface is reasonably small (i.e. if $\partial h/\partial x \ll 1.0$), the relevant equation of motion for the parison during extrusion becomes

$$\frac{\partial V_x}{\partial t} + V_x \frac{\partial V_x}{\partial x} = \frac{3}{3\rho} \frac{\partial \tau_{xx}}{\partial x} + \frac{3\tau_{xx}}{2\rho h} \frac{\partial h}{\partial x} + g_x$$

where x is the extrusion direction and h is the parison thickness. The free surface is governed by the equation

$$\frac{\partial h}{\partial t} = V_y - V_x \frac{\partial h}{\partial x}$$

and the equation of continuity yields upon integration

$$\frac{\partial h}{\partial t} = V_y - V_x \frac{\partial h}{\partial x}$$

At the free surface, both normal and shear stresses vanish. Ryan and Dutta neglect the convective terms and employ a corotational Maxwell model with parameters λ_o and η_o to obtain the following relation:

$$U_x = V_E \exp(-\alpha\lambda_o\chi) + \frac{Lg}{\lambda_o}(1-\exp(-\alpha\lambda_o\chi)$$

$$- \frac{1}{\alpha\lambda_o^2}(\alpha\lambda_o\chi + \exp(-\alpha\lambda_o\chi))$$

where

$$\alpha = \rho g_x / 3\eta_o$$

V_E is the extrusion velocity at the die exit and Lg is the length of the parison under the influence of gravity. The actual length of the parison will be somewhat between Lg and Ls, where the latter represents the length that would be obtained if only swell took place in the absence of drawdown.

In order to determine the parison behavior during inflation, Ryan and Dutta write the equations of continuity and motion in

the radial direction

$$\frac{\partial}{\partial r}(rV_r) = o$$

$$\rho\left(\frac{\partial V_r}{\partial t} + V_r \frac{\partial V_r}{\partial r}\right) = -\frac{\partial P}{\partial r} + \frac{\partial \tau_{rr}}{\partial r} + \frac{\tau_{rr}-\tau_{\theta\theta}}{r}$$

The boundary conditions relate the values of the pressure, P, at the inside and outside walls of the parison. The authors employed both a modified Zaremba-Fromm-Dewitt model recommended by Pearson and Middleman (57), as well as a modified White-Metzner fluid (10).

In most extrusion blow molding operations, especially those involving high production speeds, the melt may be considered to be isothermal throughout the parison formation and free inflation stages (59,60). Recently, a number of studies have been carried out relating to heat transfer during the cooling stage (56,59-63). Typical temperature distributions during the cooling stage are shown in Figure 17 (59). These results suggest a distribution of cooling rates in the material during solidification. This leads to a distribution of crystallinity between the outer and inner surfaces of molded bottles, which may be related to the cooling rate as shown in Figure 18 (59). The combined thermal and mechanical history of the material leads to the development of frozen stresses and orientations, in addition to the above morphological effects. Therefore, the mechanical and optical properties of blow molded articles are generally anisotropic (59,64,65).

INJECTION MOLDING

Injection molding is the most important commerical process for the manufacturing of three dimensional plastics articles. The process consists of three basic steps. During the filling stage, a viscoelastic, compressible polymer melt flows into the cavity. The walls of the cavity are maintained at a temperature significantly below the solidification temperature of the material. When the cavity is full, more melt is injected into the mold during the packing stage. This step, which takes advantage of the compressibility of the melt, causes a rapid rise of the pressure in the cavity and contributes to reducing the ultimate shrinkage of the material as a result of cooling and colidification. Cooling of the material, which starts at the beginning of the filling stage, continues throughout the cycle. In particular, after packing is complete, the cooling stage proceeds until the material has solidified to the point where it can be ejected from the cavity without damage. Subsequently, the above sequence of steps is repeated. Under normal commercial operating conditions, the filling stage represents 20-25% of the total time, packing 5%,

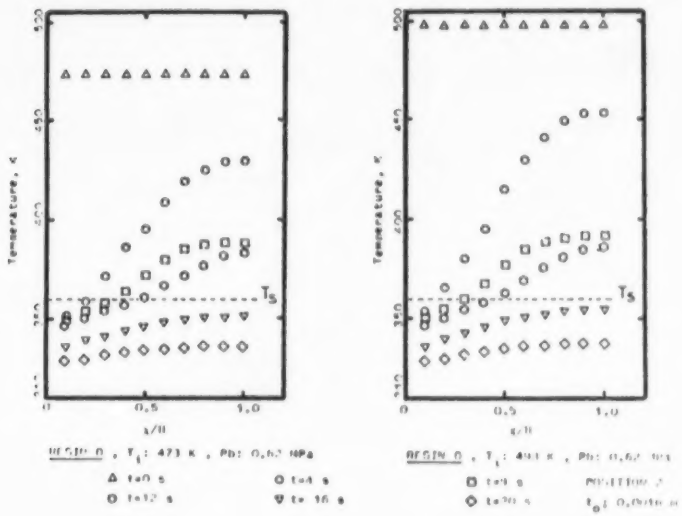

Figure 17: Temperature History During Cooling in Blow Molding of HDPE (59)

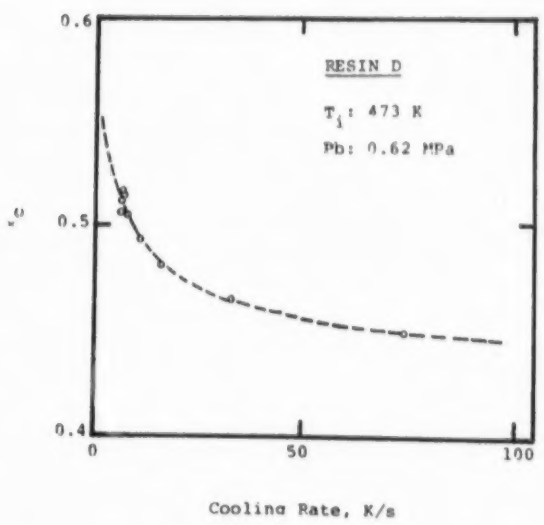

Figure 18: Crystallinity Versus Cooling Rate (59)

and cooling 70-75%. Thus, from the economic point of view, cooling is very important. However, the thermomechanical history experienced by the material during the filling and packing stages has a great influence on the ultimate behavior of the molded article. Therefore, a detailed understanding of all the steps involved in the injection molding process is essential for process and product optimization.

The early models of injection mold filling were based on simple concepts of isothermal flow of Newtonian and Power Law fluids in simple channels (e.g. circular tubes and between flat plates) (66,67,68). During the late sixties and early seventies, a number of models were developed on the basis of the solution of the transport equations for circular, semicircular, or rectangular cavities (69-82). These models usually involved Power Law fluids and one-dimensional, non-isothermal flow. In some cases, two-dimensional flow (76), elastic effects (80), latent heat effects (72) and heat of reaction (15,75) were considered. The results of these models have shown that isothermal treatment of the filling stage yields acceptable results for filling time and pressure distribution during the filling stage, in the case of thick cavities, which do not have extensive thin sections (69,70,81). Similarly, the incorporation of elastic effects does not seem to yield substantial improvements in the prediction of filling time and pressure distribution during the filling stage (80). In recent years, some commercial software packages for computer aided design/manufacturing/engineering (CAD/CAM/CAE) have been developed on the basis of analyses of the type mentioned above. These packages include CADMOLD (IKV, Aachen, West Germany) and MOLDFLOW (Colin Austin, Australia). The main utility of these models is for the prediction of filling times, pressure distributions, and short shots (7,8). They are also useful for balancing delivery channels in multi-cavity or multi-gated molding. Complex geometries may be treated as combinations of three primitive geometries: disc, circular tube, and rectangular channel.

During the last few years, more elaborate models have been proposed to deal with complex mold geometries and to elucidate, in more detail, the structure of the flow in the cavity. The model proposed by Wang et. al. (26) employs a constitutive equation developed by Leonov (83), in conjunction with both finite difference and finite element numerical schemes. The authors claim convergence of the finite element technique for quite high Deborah numbers. However, solutions have been reported for only simple flow between parallel plates.

Kamal and Lafleur (84,85) have proposed a model which incorporates the effects of fountain flow, elasticity, unsteady and inertial effects, and crystallization kinetics. The model, which employs a finite difference scheme combined with a Marker and Cell

technique, yields very good agreement with experimental data regarding the progression of the melt front and pressure distribution (Figures 19 and 20). It also yields useful information regarding the structure of the flow, especially the transverse flow near the melt front due to the fountain effect (Figure 21). The model employs a modified White-Metzner (10) constitutive equation to describe the viscoelastic behavior of the Polymer melt.

An important aspect of the mold filling process relates to the balancing of the delivery channels (sprues, runners, and gates) in the case of multi-cavity or multi-gated molds to insure equal filling times and to avoid stress imbalances in the molding. The analysis of the flow in the delivery channels may be based on the application of the above models to the melt while it flows into these channels (86). Alternatively, the analysis may be based on the step-wise or lumped application of available equations for isothermal Newtonian and non-Newtonian flow in the relevant channel geometry (5,87). Other aspects include analysis of the behavior of the melt during a pressure jump (88) or change of flow area as in the case of a step change in the cross-section of the mold (89).

In general, the treatment of the packing stage has lagged significantly behind that of the filling stage. Spencer and Gilmore (IM-1) combined an equation of state and an empirical equation for the determination of the filling time, in order to estimate the maximum pressure during packing. Kamal and Coworkers (72-75, 90) proposed simplified numerical methods for dealing with the packing stage. More recently, Kamal and Lafleur (16,84,85), have proposed a treatment based on the analysis of the unsteady, non-isothermal, compressible flow of a visco-elastic melt (White-Metzner model) into the cavity. In addition to predicting velocity and pressure distributions throughout the injection molding cycle, the model also predicts the evolution of the distributions of temperature and shear and normal stresses. For example, Figure 22 shows predictions of the distribution of shear stress as a function of time and distance from the midplane of the cavity, halfway from the gate to the far end of the cavity. Note the radical change that occurs during the packing stage and the effect of relaxation after packing, prior to solidification. Also, Figure 23 shows the distribution of normal stress, at the end of the packing stage, at various nodes (node 2 near the gate and node 25 near the far end of the cavity) as a function of the distance from the midplane.

During the cooling stage, the material solidifies. Depending on the type of material, solidification may involve only vitrification at the glass transition temperature, Tg, or it may also involve crystallization, as in the case of polyethylene. The thermomechanical history experienced by the material will lead to a

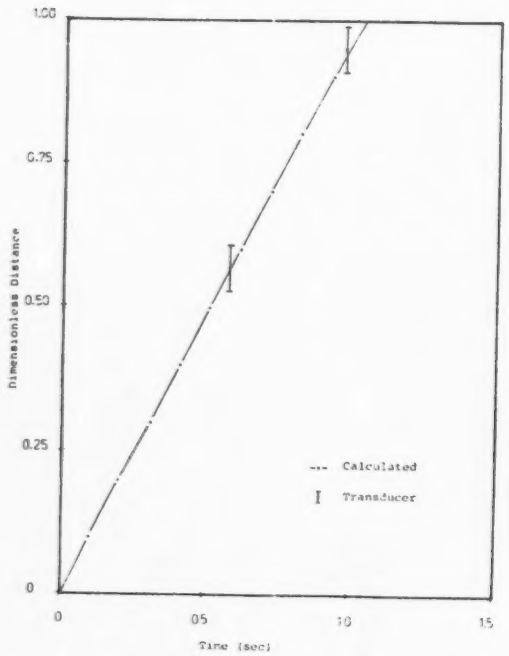

Figure 19: Progression of the melt front (85)

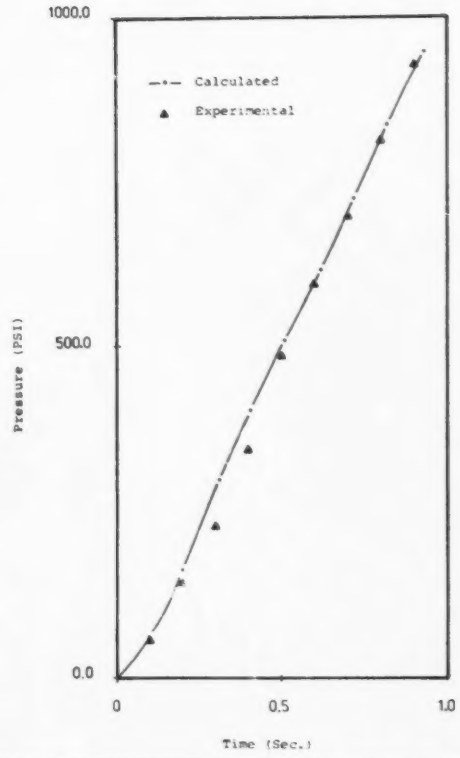

Figure 20: Pressure Variation with Time at the Entrance of the Mold (85)

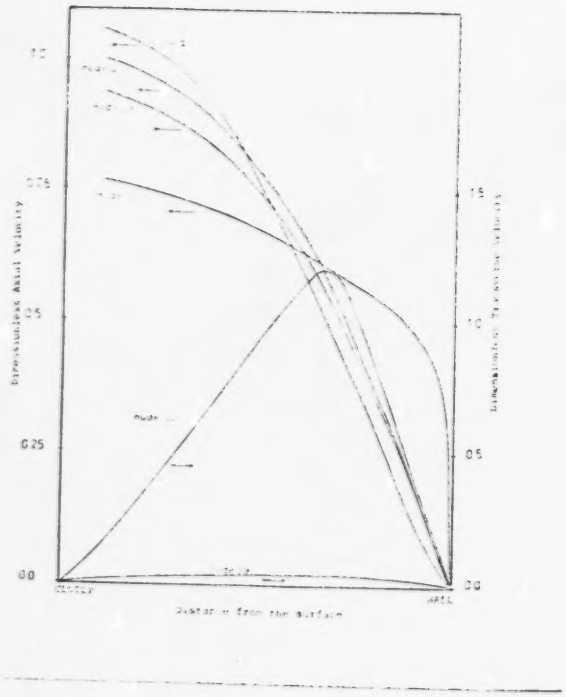

Figure 21: Axial and Transverse Velocity Distributions During Injection Mold Filling of HDPE (Fountain Flow) (85)

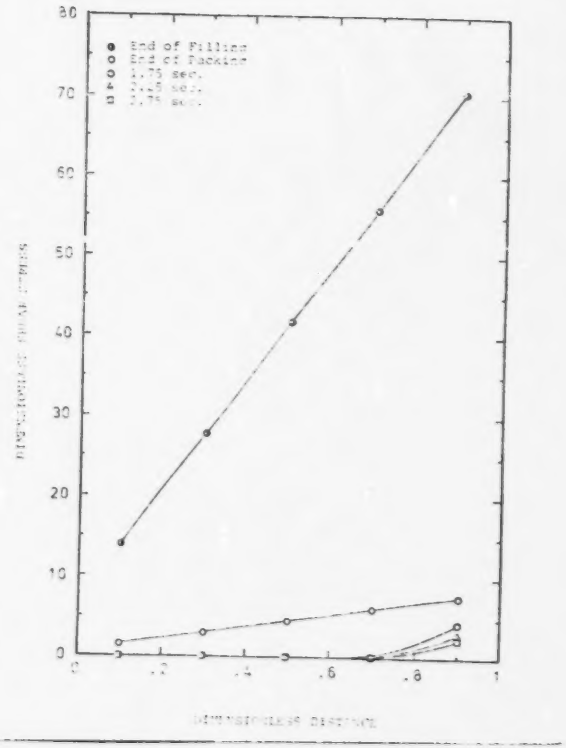

Figure 22: Variation of Shear Stress in the Cavity During Injection Molding of HDPE

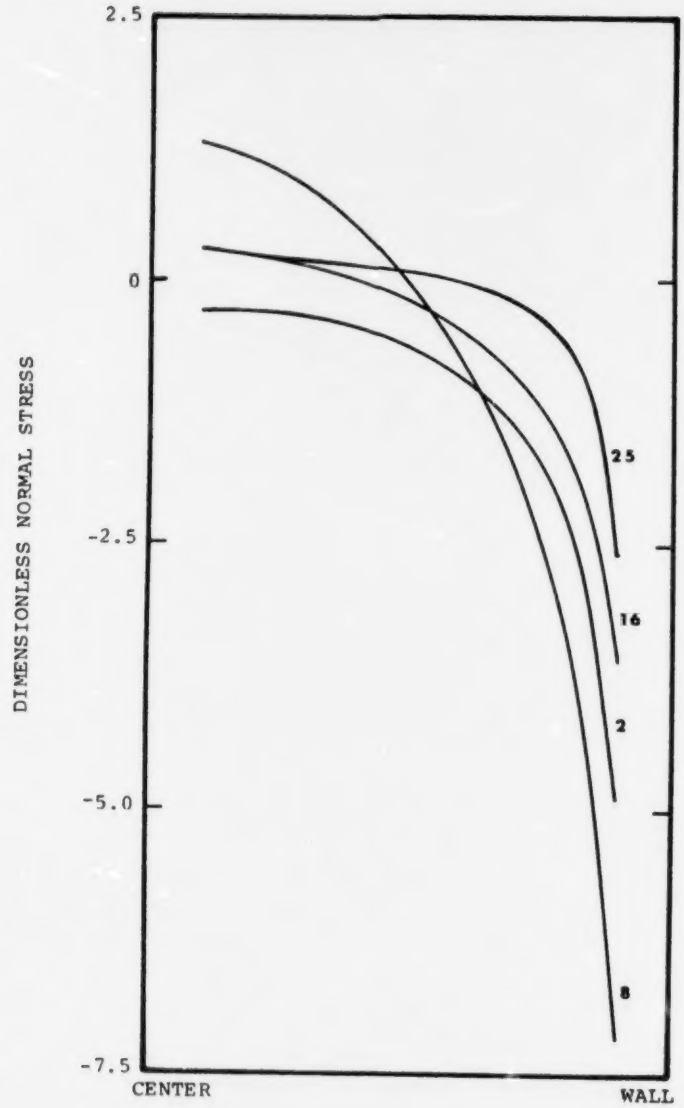

Figure 23: Normal Stress Distribution in the Cavity at the End of Packing (HDPE)

corresponding distribution of morphology, crystallinity, density, and frozen stresses or orientation in the molded article. Recent models have attempted to predict the microstructure and resulting mechanical and optical properties of the moldings, with reasonable success (80,83-85). Typical predictions of the crystallinity and amorphous birefringence in polyethylene moldings are compared to experimental results in Figures 24 and 25, respectively (85). A detailed knowledge of the distributions of crystallinity and frozen stresses (or strains) in a molding should be helpful in predicting as-molded shrinkage (91), the long term dimensional stability (e.g. warpage), and mechanical properties of the material (85,92).

REFENENCES

1. E. C. Bernhardt, "Processing of Thermoplastic Materials," Reinhold Publishing Corp., New York (1959).
2. J. M. McKelvey, "Polymer Processing," John Wiley and Sons, Inc., New York (1962).
3. J. R. A. Pearson, "Mechanical Principles of Polymer Melt Processing," Pergamon Press, Oxford (1966).
4. S. Middleman, "Fundamentals of Polymer Processing," McGraw-Hill Book Co., New York (1977).
5. J. L. Throne, "Plastics Process Engineering," Marcell Decker, Inc., New York (1979).
6. Z. Tadmor and C. Gogos, "Principles of Polymer Processing," John Wiley & Sons, New York (1979).
7. R. S. Spencer and G. D. Gilmore, J. Appl. Phys. 20:502 (1949).
8. H. Breur and G. Rehage, Kolloid Z. 216:166 (1967).
9. M. R. Kamal and N. T. LeVan, Polym. Eng. Sci. 13:131 (1973).
10. J. L. White and A. B. Metzner, J. Appl. Polym. Sci. 7:1867 (1963).
11. W. O. Criminale, Jr., J. L. Ericksen, and G. L. Filbey, Arch. Rat. Mech. Anal. 1:410 (1958).
12. A. S. Lodge, "Elastic Liquids," Academic Press, London (1964).
13. B. Bernstein, E. A. Kearsley, and L. J. Zappas, Trans. Soc. Rheol. 7:391 (1963).
14. Z. Tadmor and I. Klein, "Engineering Principles of Plasticating Extrusion," Van Nostrand Reinhold Co., New York (1970).
15. M. R. Kamal and M. E. Ryan, Polym. Eng. Sci. 20:859 (1980).
16. M. R. Kamal and P. G. Lafleur, "Heat Transfer in Injection Molding of Crystallizable Polymers," Accepted for publication, Polym. Eng. Sci. 16:1077 (1972).
17. K. Nakamura, T. Watanabe, K. Katayama, and T. Amano, J. Appl. Polym. Sci. 16:1077 (1972).
18. W. Dietz, Colloid and Polym. Sci. 259:431 (1981).
19. C. F. Huang, Ph.D. Thesis, Stevens Inst. of Technology (1978).
20. K. R. Reddy and R. I. Tanner, J. Rheol. 22:661 (1978).
21. M. J. Crochet and M. Bezy, J. Non-Newt. Fluid Mech. 5:201 (1979).

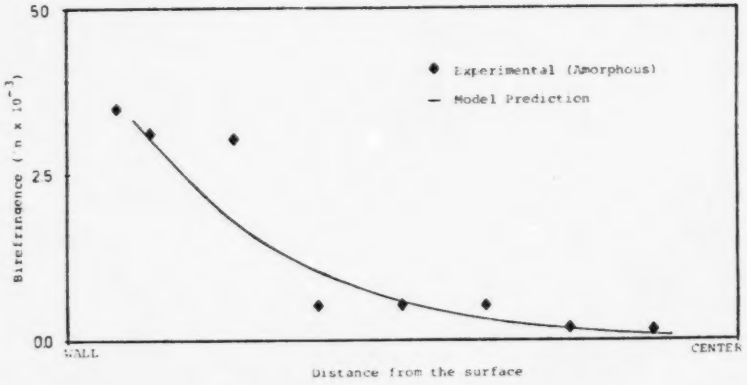

Figure 24: Experimental and Calculated Amorphous Birefringence in Injection Molded HDPE (85)

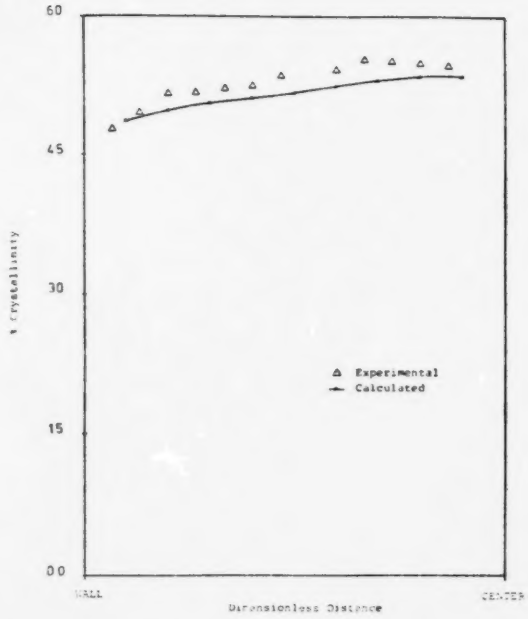

Figure 25: Gapwise Distribution of Crystallinity at the End of the Process (85)

22. M. J. Crochet and R. Keunings, J. Non-Newt. Fluid Mech. 7:199 (1980).
23. M. J. Crochet and R. Keunings, J. Non-Newt. Fluid Mech. 10: 339 (1982).
24. P.-C. Chang, T. W. Patten, and B. Finlayson, Computers and Fluids 7:285 (1979).
25. M. Viriyayuthakorn and B. Caswell, J. Non-Newt. Fluid Mech. 6:245 (1980).
26. K. K. Wang,
27. E. Mitsoulis, J. Vlachapoulos, and F. A. Mirza, "Finite Element Analysis of Isothermal and Non-Isothermal Polymer Melt Flows," Presented at IMRI/NRCC Mini-Symposium on "Mathematical Modelling of Plastics Processing and Control" Montreal (Feb. 1982).
28. R. E. Gaskell, J. Appl. Mech. 17:334 (1950).
29. C. Kiparissides and J. Vlachopoulos, Polym. Eng. Sci. 16:712 (1976).
30. W. W. Alston, Jr. and K. N. Astill, J. Appl. Polym. Sci. 17: 3157 (1973).
31. T.-S. Chung, J. Appl. Polym. Sci. 25:967 (1980).
32. J. Vlachopoulos and A. N. Hrymack, Polym. Eng. Sci. 20:725 (1980).
33. I. Brazinsky
34. J. F. Carley, in "Processing of Thermoplastic Materials," E. C. Berhardt, editor, Reinhold Publishing Corp., New York (1959).
35. C. D. Han and D. A. Rao, Polym. Eng. Sci. 20:128 (1980).
36. J. F. Carley, T. Endo, and W. B. Krantz, Polym. Eng. Sci. 19: 1178 (1979).
37. B. Vergnes, Materiaux et Techniques, p. 187 (juin-juillet 1981).
38. R. T. Fenner and J. G. Williams, Trans. J. Plast. Inst., p. 701 (Oct. 1967).
39. R. T. Fenner and F. Nadir, Polym. Eng. Sci. 19:203 (1979).
40. S. Basu, Polym. Eng. Sci. 21:1128 (1981).
41. B. Caswell and R. I. Tanner, Polym. Eng. Sci. 18:416 (1978).
42. M. R. Kamal and S. Petsalis, Unpublished results.
43. M. Viriyayuthakorn and R. V. DeBoo, SPE Tech. Papers 29:178 (1983).
44. N. Orbey, Ph.D. Thesis, McGill University (1983).
45. A. Garcia-Rejon, Ph.D. Thesis, McGill University (1980).
46. E. D. Henze and W. Wu, Polym. Eng. Sci. 13:153 (1973).
47. G. R. Cotten, Rubber Chem. Technol. 52:187 (1979).
48. D. H. Kalyon, Ph.D. Thesis, McGill University (1980).
49. C. E. Beyer and N. Sheptak, SPE Journal 21:190 (1965).
50. N. Wilson, M. Bentley, and B. Morgan, SPE Journal 26:34 (1970).

51. D. Kalyon, V. Tan, and M. R. Kamal, Polym. Eng. Sci. 20:773 (1980).
52. M. R. Kamal, D. Kalyon, and V. Tan, in "Rheology, vol. 3: Applications," edited by G. Astarita, G. Marrucci, and L. Nicolais; p. 149, Plenum Publishing Corp., New York (1980).
53. M. R. Kamal, V. Tan, and D. Kalyon, Polym. Eng. Sci. 21:331 (1981).
54. G. Ajroldi, Polym. Eng. Sci. 18:748 (1978).
55. H. Fukase, A. Iwaaki, and T. Kunio, SPE Tech. Papers 25:913 (1979).
56. M. E. Ryan and A. Dutta, Polym. Eng. Sci. 22:1075 (1982).
57. G. R. A. Pearson and S. Middleman, AIChE J. 23:714 (1977).
58. C. J. S. Petrie, Proc. Conf. on Polym. Rheol. and Plast. Processing, p. 307, The Plastics and Rubber Institute, London (1975).
59. M. R. Kamal and D. Kalyon, Polym. Eng. Sci. 23:503 (1983).
60. G. Menges, M. Kulik, and F. Rhiel, Plastverarbeiter, ___:685 (1973).
61. W. Dietz, Plastiques Modernes et Elastomeres 28:104 (1976).
62. M. F. Edwards, P. Suvanaphon, and W. Wilkinson, Polym. Eng. Sci. 19:911 (1979).
63. M. F. Edwards, S. Georghiades, and P. K. Suvanaphen, Plast. Rubber Processing Applications 1:162 (1981).
64. J. L. White and A. Agarwal, Polym. Eng. Rev. 1:267 (1981).
65. M. Cakmak, J. Spruiell, and J. L. White, SPE Tech. Papers 29: 394 (1983).
66. R. S. Spencer and G. D. Gilmore, J. Colloid Sci. 6:118 (1951).
67. R. L. Ballman, T. Shusman, and H. L. Toor, Ind. Eng. Chem. 51: 847 (1959).
68. R. B. Staub, SPE Journal 17:345 (1961).
69. D. H. Harry and R. G. Parrott, Polym. Eng. Sci. 10:209 (1970).
70. J. L. Berger and C. G. Gogos, Polym. Eng. Sci. 13:102 (1973).
71. P. C. Wu, C. F. Huang, and C. G. Gogos, Polym. Eng. Sci. 14: 223 (1974).
72. M. R. Kamal and S. Kenig, Polym. Eng. Sci. 12:294 (1972).
73. M. R. Kamal and S. Kenig, Polym. Eng. Sci. 12:302 (1972).
74. M. R. Kamal, Y. Kuo, and P. H. Doan, Polym. Eng. Sci. 15:863 (1975).
75. M. E. Ryan, Ph.D. Thesis, McGill University (1978).
76. E. Broyer, C. Gutfinger, and Z. Tadmor, Trans. Soc. Rheol. 19:423 (1975).
77. J. L. White, Polym. Eng. Sci. 15:44 (1975).
78. H. A. Lord and G. Williams, Polym. Eng. Sci. 15:569 (1975).
79. Y. Kuo and M. R. Kamal, AIChE J. 22:661 (1976).
80. K. K. Wang, et. al., Injection Molding Project, College of Engineering, Cornell University, Progress Report #6 (1979).
81. C. F. Huang, C. G. Gogos, and L. Schmidt, Paper 94e, 71st Annual AIChE Meeting, November 15, 1978.
82. M. E. Ryan and T.-S. Chung, Polym. Eng. Sci. 18:642 (1980).
83. A.I. Leonov, Rheol. Acta 15:85 (1976).

84. M. R. Kamal and P. G. Lafleur, Polym. Eng. Sci. 22:1066 (1982).
85. M. R. Kamal and P. G. Lafleur, SPE Tech. Papers, 29:386 (1983).
86. V. W. Wang, K. K. Wang, and C. A. Hieber, SPE Tech. Papers, 29: 663 (1983).
87. C. A. Hieber, R. K. Upadhyay, and A. I. Isayev, SPE Tech. Papers 29:698 (1983).
88. A. I. Isayev, SPE Tech. Papers 29:710 (1983).
89. R. K. Upadhyay and A. Isayev, SPE Tech. Papers 29:714 (1983).
90. Y. Kuo and M. R. Kamal, in "Science and Technology of Polymer Processing," edited by N. P. Suh and N.-H. Sung, p. 329, The M.I.T. Press, Cambridge, Mass. (1979).
91. W. B. Hoven-Nievelstein and G. Menges, SPE Tech. Papers 29: 737 (1983).
92. M. R. Kamal and F. H. Moy, Chem. Eng. Commun. 12:253 (1981).

APPENDIX

Parameters of Constitutive Equations for Two-Dimensional Flow

As indicated in the above discussion, there is a growing tendency to analyze polymer shaping operations in terms of two-dimensional viscoelastic flow. The convected Maxwell fluid, the White-Metzner model, and the CEF fluid are among those commonly employed in dealing with such problems. Also, they have been employed in some of the analyses discussed in this manuscript. Therefore, we list below the important parameters for two-dimensional flow for these models.

Convected Maxwell fluid (27):

$$\tau_{xx} + \lambda \left[V_x \frac{\partial \tau_{xx}}{\partial x} + V_y \frac{\partial \tau_{xx}}{\partial y} - 2 \frac{\partial V_x}{\partial x} \tau_{xx} - 2 \frac{\partial V_x}{\partial y} \right] = 2\eta \frac{\partial V_x}{\partial x}$$

$$\tau_{yy} + \lambda \left[V_x \frac{\partial \tau_{yy}}{\partial x} + V_y \frac{\partial \tau_{yy}}{\partial y} - 2 \frac{\partial V_y}{\partial y} \tau_{yy} - 2 \frac{\partial V_y}{\partial x} \tau_{xy} \right] = 2\eta \frac{\partial V_y}{\partial y}$$

$$\tau_{xy} + \lambda \left[V_x \frac{\partial \tau_{xy}}{\partial x} + V_y \frac{\partial \tau_{xy}}{\partial y} - \frac{\partial V_y}{\partial x} \tau_{xx} - \frac{\partial V_x}{\partial y} \tau_{yy} \right] = \eta \left(\frac{\partial V_y}{\partial x} + \frac{\partial V_x}{\partial y} \right)$$

CEF equation (Ψ_1, Ψ_2 are normal stress coefficients) (27):

$$\tau_{xx} = 2\eta \frac{\partial V_x}{\partial x} + (\tfrac{1}{2}\Psi_1 + \Psi_2)(\gamma_{xx}^2 + \gamma_{xy}^2) - \tfrac{1}{2}\Psi_1\left[(V_x \frac{\partial \gamma_{xx}}{\partial x} + \frac{\partial \gamma_{xx}}{\partial y}) - \gamma_{xy}(\frac{\partial V_x}{\partial y} - \frac{\partial V_y}{\partial x})\right]$$

$$\tau_{yy} = 2\eta \frac{\partial V_y}{\partial y} + (\tfrac{1}{2}\Psi_1 + \Psi_2)(\gamma_{yy}^2 + \gamma_{xy}^2) - \tfrac{1}{2}\Psi_1\left[(V_x \frac{\partial \gamma_{yy}}{\partial x} + V_y \frac{\partial \gamma_{yy}}{\partial y}) - \gamma_{xy}(\frac{\partial V_x}{\partial y} - \frac{\partial V_y}{\partial x})\right]$$

$$\tau_{xy} = \eta(\frac{\partial V_y}{\partial x} + \frac{\partial V_x}{\partial y}) + (\tfrac{1}{2}\Psi_1 + \Psi_2)\left[\gamma_{xy}(\gamma_{xx} + \gamma_{yy})\right] - \tfrac{1}{2}\Psi_1\left[(V_x \frac{\partial \gamma_{xy}}{\partial x} + V_y \frac{\partial \gamma_{xy}}{\partial y}) + \tfrac{1}{2}(\gamma_{xx} - \gamma_{yy})(\frac{\partial V_x}{\partial y} - \frac{\partial V_y}{\partial x})\right]$$

where

$$\gamma_{xx} = 2 \frac{\partial V_x}{\partial x}\ ,\ \gamma_{yy} = 2 \frac{\partial V_y}{\partial y} \text{ and } \gamma_{xy} = \frac{\partial V_y}{\partial x} + \frac{\partial V_x}{\partial y}$$

White-Metzner Model

$$\tau_{xx} + \frac{\eta}{G}(\frac{\partial \tau_{xx}}{\partial t} + V_x \frac{\partial \tau_{xx}}{\partial x} + V_y \frac{\partial \tau_{xx}}{\partial y} - 2 \frac{\partial V_x}{\partial x} \tau_{xy} - 2 \frac{\partial V_x}{\partial y} \tau_{xy}) = 2\eta \frac{\partial V_x}{\partial x}$$

$$\tau_{yy} = \frac{\eta}{G}(\frac{\partial \tau_{yy}}{\partial t} + V_x \frac{\partial \tau_{yy}}{\partial x} + V_y \frac{\partial \tau_{yy}}{\partial y} - 2 \frac{\partial V_y}{\partial x} \tau_{xy} - 2 \frac{\partial V_y}{\partial y} \tau_{xy}) = 2\eta \frac{\partial V_y}{\partial y}$$

$$\tau_{xz} + \frac{\eta}{G}\left(\frac{\partial \tau_{xy}}{\partial t} + u\frac{\partial \tau_{xy}}{\partial x} + v\frac{\partial \tau_{xy}}{\partial y} - \frac{\partial V_x}{\partial y}\tau_{yy} - \frac{\partial V_y}{\partial x}\tau_{xx}\right)$$

$$= \eta\left(\frac{\partial V_x}{\partial y} + \frac{\partial V_y}{\partial x}\right)$$

The second invariant of the rate of deformation tensor is

$$\vec{\vec{\Delta}} : \vec{\vec{\Delta}} = 4\left(\frac{\partial V_x}{\partial x}\right)^2 + 2\left(\frac{\partial V_x}{\partial y} + \frac{\partial V_y}{\partial x}\right)^2 + 4\left(\frac{\partial V_y}{\partial y}\right)^2$$